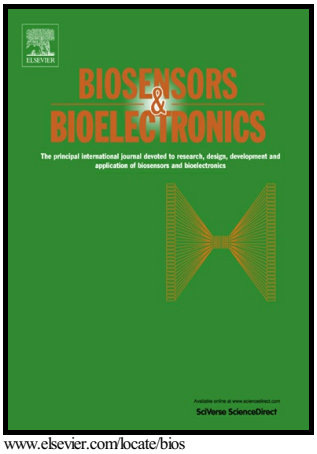

www.elsevier.com/locate/bios

A novel ECL biosensor for the detection of concanavalin A based on glucose functionalized $NiCo_2S_4$ nanoparticles-grown on carboxylic graphene as quenching probe

Xiaojian Li, Yaoguang Wang, Li Shi, Hongmin Ma, Yong Zhang, Bin Du, Dan Wu, Qin Wei

PII: S0956-5663(17)30309-3
DOI: http://dx.doi.org/10.1016/j.bios.2017.04.050
Reference: BIOS9711

To appear in: *Biosensors and Bioelectronic*

Received date: 18 January 2017
Revised date: 27 April 2017
Accepted date: 29 April 2017

Cite this article as: Xiaojian Li, Yaoguang Wang, Li Shi, Hongmin Ma, Yong Zhang, Bin Du, Dan Wu and Qin Wei, A novel ECL biosensor for the detection of concanavalin A based on glucose functionalized $NiCo_2S_4$ nanoparticles-grow on carboxylic graphene as quenching probe, *Biosensors and Bioelectronic* http://dx.doi.org/10.1016/j.bios.2017.04.050

A novel ECL biosensor for the detection of concanavalin A based on glucose functionalized $NiCo_2S_4$ nanoparticles-grown on carboxylic graphene as quenching probe

Xiaojian Li, Yaoguang Wang, Li Shi, Hongmin Ma, Yong Zhang, Bin Du, Dan Wu* and Qin Wei

Key Laboratory of Chemical Sensing & Analysis in Universities of Shandong, School of Chemistry and Chemical Engineering, University of Jinan, Jinan 250022, PR China

*** Corresponding author**

Tel.: +86 531 82767872;

Fax: +86 531 82765969;

E-mail: wudan791108@163.com

Abstract

An electrochemiluminescence (ECL) biosensor was developed for detection of Concanavalin A (Con A). Chitosan/$Ru(bpy)_3^{2+}$/silica/Fe_3O_4 nanomaterials (CRuSi-Fe_3O_4) were synthesized through W/O microemulsion route. The added Fe_3O_4 nanoparticles can simplify the prepared process and enhance the conductivity of nanomaterials which can increase the ECL intensity of luminophor CRuSi-Fe_3O_4. In addition, the layered structure of CRuSi-Fe_3O_4 can immobilize lots of Con A using glutaraldehyde as the coupling agent which can improve the sensitivity of the biosensor. Then the quenching probe glucose functionalized $NiCo_2S_4$ nanoparticles-grown on carboxylic graphene ($NiCo_2S_4$-COOH-rGO@Glu) was anchored on the modified-electrode via the specific carbohydrate-Con A interaction. Here, $NiCo_2S_4$ was used to quench the ECL of CRuSi-Fe_3O_4, graphene was used to grow $NiCo_2S_4$ nanoparticles as carrier materials and glucose was served as the recognition element for bounding Con A. Therefore, a desirable quenching ECL signal was measured with $S_2O_8^{2-}$ as the coreactant of CRuSi-Fe_3O_4. Under the optimization of determination conditions, a linear response range for Con A from 0.5 pg mL^{-1} to 100 ng mL^{-1} was obtained, and the detection limit was calculated to be 0.18 pg mL^{-1} (S/N=3).

Key words: electrochemiluminescence biosensor ; quenching; Chitosan/$Ru(bpy)_3^{2+}$/silica/Fe_3O_4 nanomaterials; glucose functionalized $NiCo_2S_4$ nanoparticles-grown on carboxylic graphene; specific carbohydrate-Con A interaction

1. Introduction

Concanavalin A (Con A), is a legume protein, which is extracted from jack bean by the method of Sumner and Howell in 1936. Con A exists as a dimmer below pH 5.5 and tetramer between pH 5.8 and pH 7.0, and each subunit of Con A possesses four binding sites under the neutral conditions (Liu et al. 2014). Con A exhibits some unusual biological properties because of its ability to bind various carbohydrates such as mannose, glucose and some glycoproteins, such as horseradish peroxidase (HRP) and glucose oxidase (GOD) (Yu et al. 2017). On account of the biospecific carbohydrate-lectin interactions, Con A is recently chosen as protein model for deeply studying the molecules recognition or biological processes, which are important for clinical diagnostics and drug development, for instance, the detection of cancer cell and leukemia cell (Li et al. 2016b). Therefore, it is significant to develop a new method for sensing Con A. Many approaches have been developed to detect Con A because it is an important target for studying the carbohydrate-protein interactions, such as fluorescence technique (Huang et al. 2009), surface plasmon resonance (Huang et al. 2013), UV-vis spectra (Hone et al. 2003) and electrochemical method (Loaiza et al. 2011). In this work, a quenching ECL biosensor was developed based on chitosan/$Ru(bpy)_3^{2+}$/silica/Fe_3O_4 nanomaterials (CRuSi-Fe_3O_4) as luminophor and glucose functionalized $NiCo_2S_4$ nanoparticles-grown on carboxylic graphene ($NiCo_2S_4$-COOH-rGO@Glu) as quenching probe.

Magnetic nanomaterials (such as Fe_3O_4) have been extensively studied and used in magnetic resonance imaging, drug delivery, biological separation and biological

catalysis (Wei and Wang 2008). In this work, Fe_3O_4 was used to immobilize $Ru(bpy)_3^{2+}$ which can simplify separation process. As a conventional ECL reagent, $Ru(bpy)_3^{2+}$ has several advantages, such as chemical stability, high ECL efficiency and superior biocompatibility in ECL bioanalytical system (Ma et al. 2014; Sardesai et al. 2011; Zhu et al. 2010). The approaches of immobilized $Ru(bpy)_3^{2+}$ have been developed in fabricating biosensors, such as ion exchanger Nafion (Guo and Dong 2004), layer-by layer method with negatively charged nanoparticles (Guo et al. 2004) and covalent attachment (Greenway et al. 2006) (Zhou et al. 2014). In this work, chitosan/$Ru(bpy)_3^{2+}$/silica nanomaterials (CRuSi) with stable ECL signals were synthesized by a typical W/O reverse microemulsion system according to the literature (Dennany et al. 2003). In addition, Fe_3O_4 was added during the reaction, then Fe_3O_4 was covered by the layered silica and $Ru(bpy)_3^{2+}$. The magnetic nanomaterials CRuSi-Fe_3O_4 had high efficiency and stable ECL signal. $NiCo_2S_4$-COOH-rGO was used as quenching probe in the ECL biosensor for ultrasensitive detection of Con A. Via a facile one-pot solvothermal method, the hybrid of $NiCo_2S_4$ nanoparticles in situ grown on N and S codoped graphene was synthesized from metal salts, thiourea, and carboxylic graphene oxide in the medium of ethylene glycol (Liu et al. 2013). To specific bind Con A, glucose was used to functionalize $NiCo_2S_4$-COOH-rGO. Mallakpour et al. synthesized glucose functionalized multi-walled carbon nanotubes (CNTs) using a covalent, non-specific functionalization approach (Mallakpour and Zadehnazari 2013). In covalent functionalization, CNTs were functionalized by irreversible attachment of appendage

on the sidewalls and/or on the tips (Wu et al. 2012). According to this method, glucose can be immobilized on the surface of carboxylic graphene.

In this work, a powerful and stable sensing platform based on enhanced ECL CRuSi-Fe_3O_4 for Con A detection was established by the quenching of $NiCo_2S_4$-COOH-rGO@Glu. The detailed fabrication process of the proposed biosensor was exhibited in Fig. 1b. Initially, CRuSi-Fe_3O_4 was drop-coated on glass carbon electrode (GCE). Subsequently, Con A was immobilized on the modified GCE through chitosan adsorbing proteins. The nonspecific binding sites on electrode were blocked with bovine serum albumin (BSA). Following which, $NiCo_2S_4$-COOH-rGO@Glu employing as the efficient quenching probe was incubated with the modified-GCE, and a remarkable ECL response was obtained for quantitative detection of Con A. The details of the preparation, characterization, optimization of conditions and the response performances of the biosensor are as followings.

2. Experimental section

2.1. Materials

Concanavalin A (Con A) and bovine serum albumin (BSA) (96%-99%) were purchased from Aladdin Industrial Corporation (Shanghai, China). $Ru(bpy)_3Cl_2$ was purchased from TOKYO Chemical Industry CO. LTD. (Tokyo, Japan). Chitosan, glucose, glutaraldehyde, ethylene glycol (EG), triton X-100, tetraethylorthosilicate (TEOS, 99%), triethylamine, 1-hexanol, cyclohexane,

(3-aminopropyl)-triethoxysilane, ammonium hydroxide, N,N'-carbonyldiimidazole (CDI), acetone and ethanol were obtained from Sinopharm Chemical. All other chemicals were of analytical reagent grade and were used without further purification. Phosphate buffered saline (PBS) was prepared by using 1/15 mol·L^{-1} Na_2HPO_4 and 1/15 mol·L^{-1} KH_2PO_4 solution. 2.5 mM $K_3Fe(CN)_6$/$K_4Fe(CN)_6$ and 0.1 M KNO_3 solution were used as electrolyte for electrochemical impedance spectroscopy (EIS). Ultrapure water (18.25 MΩ cm, 24 ˚C) was used for all of the experiments. Chitosan was dissolved in 1% acetic acid.

2.2. Apparatus

Scanning electron microscope (SEM) images and Energy dispersive spectrometer (EDS) were obtained using a field emission SEM (Zeiss, Germany). The ECL measurements were performed with a MPI-F flow-injection chemiluminescence detector (Xi'an remax Electronic Science Tech. Co. Ltd., China) and electrochemical measurements were carried out on CHI760D electrochemical workstation (Chenhua Instrument Shanghai Co., Ltd, China) using a three-electrode system consisted of a platinum wire as an auxiliary electrode, an Ag/AgCl electrode as reference electrode, and GCE (4 mm in diameter) as working electrode.

2.3. Preparation of CRuSi-Fe_3O_4 nanomaterials

Fe_3O_4 nanoparticles was prepared as described previously with some slight modifications (Wang et al. 2013) and the detail process was supported in Supplementary Material. The W/O reverse microemulsion system (Dang et al. 2014)

was prepared first by mixing 1.77 mL of TX-100, 7.5 mL of cyclohexane, 1.8 mL of 1-hexanol and 1 mL of 50 mg mL^{-1} Fe_3O_4 solution. Then 5 mL of 10 mM $Ru(bpy)_3^{2+}$ aqueous solution and 100 μL of 0.5% chitosan were added into the mixture. In the presence of 150 μL TEOS, a polymerization reaction was initiated by adding 1 mL NH_4OH (25%-28%). The hydrolysis reaction was allowed to continue for 24 h. Then acetone was added to destroy the emulsion, followed by centrifuging and washing with ethanol and water. At last, CRuSi-Fe_3O_4 was obtained and dispersed in 0.5% chitosan.

2.4. Preparation of $NiCo_2S_4$-COOH-rGO@Glu

Graphene oxide (GO) was prepared by a modified Hummers' method from graphite powder (Marcano et al. 2010) and the detailed experiment process was showed in Supplementary Material. To obtain carboxylic graphene oxide (COOH-GO), GO was dispersed in 100 mL 5% HCl and refluxed for 12 h at 120 ˚C. After naturally cooling to room temperature, the refluxed product was centrifuged and washed with ultrapure water until pH reached 7. The final product was vacuum dried at 35 ˚C for 12 h to obtain COOH-GO.

$NiCo_2S_4$-COOH-rGO was prepared as described previously with some slight modifications (Liu et al. 2013). Briefly, 0.0747 g $Co(OAc)_2$ and 0.0373 g $Ni(OAc)_2$ were dissolved in 30 mL of 50 mg mL^{-1} GO/EG suspension with stirring at 80 °C for 2 h. Then, 0.0685 g thiourea was added into the above mixture, then transferred the mixture to a Teflon reaction kettle and heated at 200 ˚C for 6 h. The resulted product

was collected by centrifuging and washing with ethanol and water. The finally product was vacuum dried at 35 ˚C for 12 h.

The synthetic process of $NiCo_2S_4$-COOH-rGO@Glu was displayed in Fig. 1a. Firstly, 50 mg $NiCo_2S_4$-COOH-rGO was dispersed in 10 mL of 10 mg mL^{-1} CDI aqueous solution and ultrasonicated for 1 h, then stirred for 12 h at room temperature. Subsequently, 100 mg glucose was added in the above mixture. The reaction was allowed to proceed at room temperature for 12 h. The resulted product was collected by centrifuging and washing with ethanol and water and finally vacuum dried at 35 ˚C for 12 h, obtaining $NiCo_2S_4$-COOH-rGO@Glu. Following which, 3 mg $NiCo_2S_4$-COOH-rGO@Glu was dispersed in 1 mL PBS (pH 7.4), then 500 μL of 1% BSA was added to the mixture for about 6 h to block the non-specific adsorption sites. At last, $NiCo_2S_4$-COOH-rGO@Glu was collected by centrifugation and redispersed in 1 mL PBS (pH 7.4), then stored at 4 °C when not used.

2.5. Fabrication of the biosensor for detecting Con A

Before modification, GCE was polished to a mirror-like surface using alumina powder (1.0, 0.3 and 0.05 μm) and thoroughly cleaned with ultrapure water. After that, 6 μL of 3 mg mL^{-1} CRuSi-Fe_3O_4 dispersion was dropped on the pretreated GCE and dried in air. Subsequently, 10 μL various concentrations of Con A were incubated on the modified GCE and dried at 4 ˚C. In this step, Con A would be captured by covalent cross-linking (Yang et al. 2009) and glutaraldehyde was used to activate the surface amino group of chitosan and Con A. During the fabrication of the biosensor, for each modification step, the electrode was washed with ultrapure water to eliminate

the nonspecific binding. Then, 3 μL of 1% BSA solution for 1 h to block nonspecific binding sites. Finally, the modified electrode was incubated with 3 μL of 3 mg mL^{-1} $NiCo_2S_4$-COOH-rGO@Glu through a carbohydrate-Con A interaction for 2 h at 4 ˚C.

2.6. ECL detection of Con A

The ECL measurement was performed in 10 mL PBS (pH 8.0) containing 0.1 M KCl and 0.1 M $K_2S_2O_8$ with a scanned potential (-1.8 to 0 V) at the scan rate of 0.1 V s^{-1}. The voltage of the photomultiplier tube (PMT) was set as 750 V.

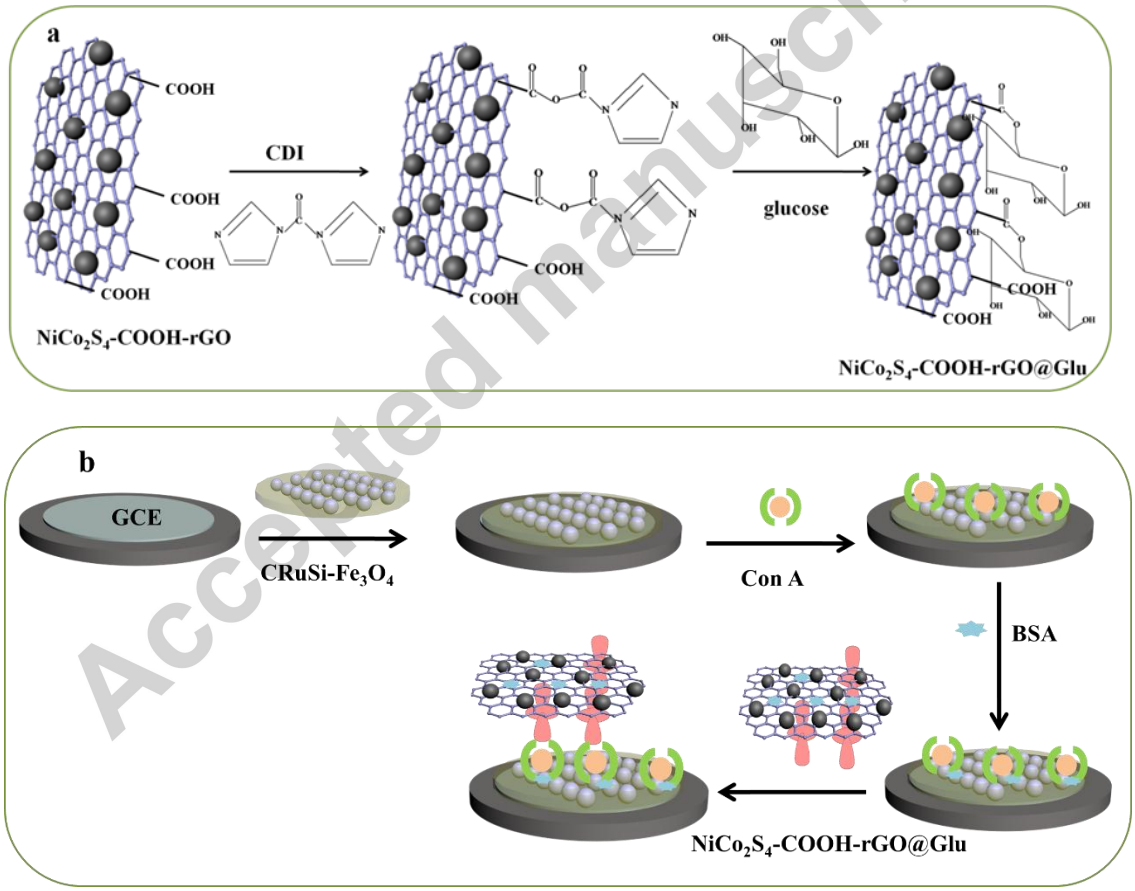

Fig. 1 The illustration of the synthetic process of $NiCo_2S_4$-COOH-rGO@Glu (a) and the fabricated process of the developed biosensor (b).

3 Results and discussion

3.1. Characterization of Fe_3O_4, CRuSi-Fe_3O_4, COOH-GO and $NiCo_2S_4$-COOH-rGO

The morphologies of Fe_3O_4, CRuSi-Fe_3O_4, COOH-GO and $NiCo_2S_4$-COOH-rGO were investigated by SEM (Fig. 2). Fe_3O_4 nanoparticles were generally spherical ones with mean diameter of approximately 250 nm and their surfaces of Fe_3O_4 nanoparticles were rather rough with multiple bulges, as shown in Fig. 2A. As for CRuSi-Fe_3O_4, we can see that CRuSi-Fe_3O_4 displayed layered structure and Fe_3O_4 was coated by SiO_2, chiotsan and $Ru(bpy)_3^{2+}$ from Fig. 2B. Fig. 2C was the EDS of CRuSi-Fe_3O_4 which displayed the main elements of nanomaterials containing Fe, O, Si and Ru. The ECL results indicated that CRuSi-Fe_3O_4 had high ECL efficiency though the elements of Ru in CRuSi-Fe_3O_4 occupied only 0.1%. To further investigate $Ru(bpy)_3^{2+}$ successfully doped in nanomaterials, the UV-vis of Fe_3O_4 (a), $Ru(bpy)_3^{2+}$ (b) and CRuSi-Fe_3O_4 (a) was measured shown in Fig. S1 (Supplementary material). No obvious adsorption peak was observed for Fe_3O_4 nanoparticles. $Ru(bpy)_3^{2+}$ displayed a characteristic peak at about 450 nm and the characteristic peak was also shown in CRuSi-Fe_3O_4, which proved CRuSi-Fe_3O_4 successfully synthesized. In addition, the XRD of Fe_3O_4 (curve a) and CRuSi-Fe_3O_4 (curve b) was investigated in Fig. S2 (Supplementary material). The XRD of Fe_3O_4 showed six diffraction peaks which were indexed as (220), (311), (400), (422), (551) and (440), respectively, indicating Fe_3O_4 had been successfully constructed (Wang et al. 2013). As for CRuSi-Fe_3O_4, these six peaks still observed which meant that Fe_3O_4 had been well

preserved after a series of procedures. Fig. 2D was the SEM images of COOH-GO and it displayed flake-like shaped. SEM images (Fig. 2E) and the EDS (Fig. 2F) of the synthesized $NiCo_2S_4$-COOH-rGO clearly revealed that metal sulfide nanoparticles were uniformly decorated on graphene sheets without aggregation. The SEM images of pure CoS were also characterized shown in Fig. S3 (Supplementary material) and CoS particles aggregated each other creating clumps. During the reaction of $NiCo_2S_4$-COOH-rGO, EG acted as a mild reductant to get reduced graphene oxide (rGO) and also the solvent with a chelating effect, which avoided agglomeration of nanoparticles. GO provided large amounts of defects/functional groups as nucleation sites for in situ growth of $NiCo_2S_4$ nanoparticles (Qiao et al. 2013). After glucose functionalized $NiCo_2S_4$-COOH-rGO, the thickness of graphene slightly increased, indicating that $NiCo_2S_4$-COOH-rGO@Glu was successfully synthesized, as shown in Fig. S4.

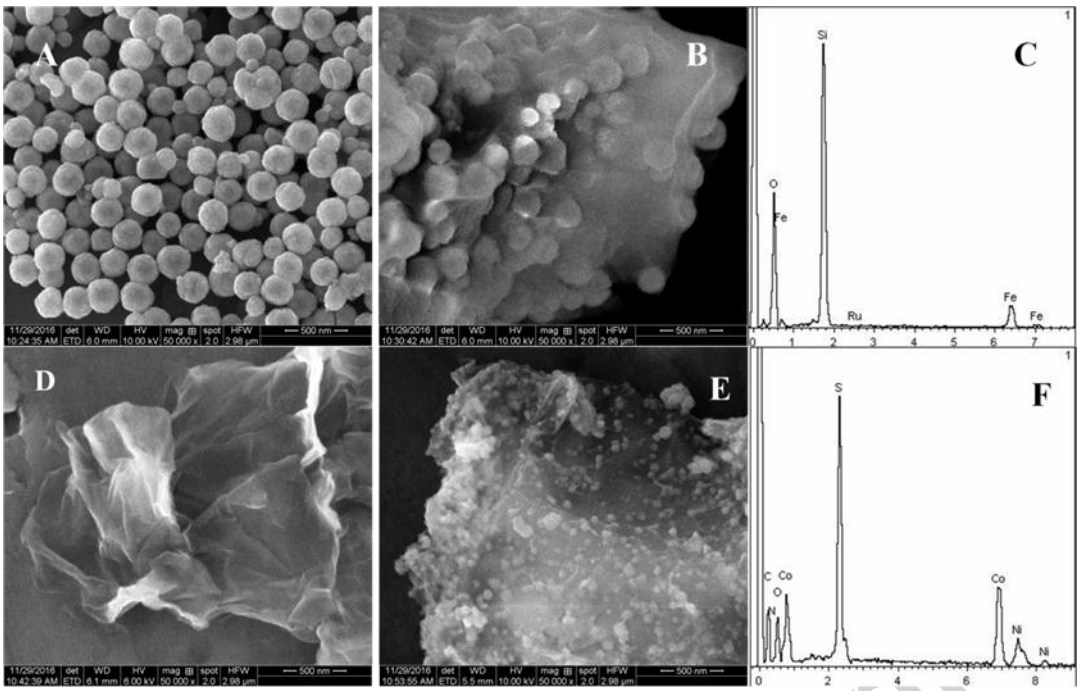

Fig. 2 SEM image of Fe_3O_4 (A), CRuSi-Fe_3O_4 (B), COOH-rGO (D) and $NiCo_2S_4$-COOH-rGO (E); EDS of CRuSi-Fe_3O_4 (C) and $NiCo_2S_4$-COOH-rGO (F).

Cyclic voltammetry (CV) of $NiCo_2S_4$-COOH-rGO, $NiCo_2S_4$-COOH-rGO@Glu and CRuSi-Fe_3O_4 was measured in PBS with (Fig. 3A) or without (Fig. S5, Supplementary material) $K_2S_2O_8$. As shown in Fig. 3A, bare GCE had an obvious reduction peak at -1.0 V (curve a) which was attributed to $K_2S_2O_8$. After CRuSi-Fe_3O_4 modified-GCE, the reduction peak shifted to -0.89 V (curve b), indicating that $S_2O_8^{2-}$ could be more favorably electro-reduced on the CRuSi-Fe_3O_4 (eq 1) (Cheng et al. 2012b; Zhang et al. 2016a). This is mainly because the conductivity of CRuSi-Fe_3O_4 catalyzed the electro-reduction of $S_2O_8^{2-}$. Compared to the CV of bare GCE (curve a), the larger cathodic current indicate electron injection process shown in eq 2a. When $NiCo_2S_4$-COOH-rGO was modified on the surface of GCE (curve c), the reduction peak shifted to -0.92 V and the current of reduction peak remarkably decreased. In

addition, a weak oxidation peak was also displayed at -0.29 V which mainly induced the quench of CRuSi-Fe_3O_4. The CV of $NiCo_2S_4$-COOH-rGO/CRuSi-Fe_3O_4/GCE (curve d) maintained its reduction peak at about -0.92 V. The electrochemistry behavior of $NiCo_2S_4$-COOH-rGO was investigated in PBS without coreactant $K_2S_2O_8$. As shown in Fig. S5, bare GCE had no oxidation and reduction peak (curve a). Curve b was the CV of $NiCo_2S_4$-COOH-rGO and an obvious oxidation peak was shown at -0.34 V, indicating that Co(II) and Ni(II) can release electron producing Co(III) and Ni(III), respectively. After glucose functionalized $NiCo_2S_4$-COOH-rGO (curve c), compared to $NiCo_2S_4$-COOH-rGO, the current of oxidation peak at -0.23 V increased. However, CRuSi-Fe_3O_4 had no obvious oxidation and reduction peak (curve d). The oxidation peak of $NiCo_2S_4$-COOH-rGO/CRuSi-Fe_3O_4/GCE (curve e) shifted to -0.28 V comparing to $NiCo_2S_4$-COOH-rGO/GCE (curve b).

3.2. ECL mechanism of CRuSi-Fe_3O_4/$K_2S_2O_8$ system and $NiCo_2S_4$-COOH-rGO quenching CRuSi-Fe_3O_4

The ECL spectra of $Ru(bpy)_3^{2+}$ (A) and CRuSi-Fe_3O_4 (B) was investigated, as shown in Fig. S6. The characterization peak of $Ru(bpy)_3^{2+}$ was at 650 nm and the characterization peak of CRuSi-Fe_3O_4 was at about 670 nm, indicating that the main luminescent composition of CRuSi-Fe_3O_4 was $Ru(bpy)_3^{2+}$. Therefore, the ECL mechanism of CRuSi-Fe_3O_4/$K_2S_2O_8$ system in this work was similar with $Ru(bpy)_3^{2+}$/$K_2S_2O_8$ system which was investigated in our previous work (Li et al. 2016a). In short, there was at least two parallel pathways to activate the $Ru(bpy)_3^{2+}$ to

its excited states. The ECL excitation route of $Ru(bpy)_3^{2+}$ could occur by reduction-initiated oxidative excitation pathway (reactions (2a) and (2b)) or the oxidation-initiated reductive excitation pathway (reactions (3a) and (3b)) as follows:

$$S_2O_8^{2-} + e^- \rightarrow SO_4^{2-} + SO_4^{\bullet-} \quad (1)$$

$$Ru(bpy)_3^{2+} + e^- \rightarrow Ru(bpy)_3^{+} \quad (2a)$$

$$Ru(bpy)_3^{+} + SO_4^{\bullet-} \rightarrow Ru(bpy)_3^{2+*} + SO_4^{2-} \quad (2b)$$

$$Ru(bpy)_3^{2+} + SO_4^{\bullet-} \rightarrow Ru(bpy)_3^{3+} + SO_4^{2-} \quad (3a)$$

$$Ru(bpy)_3^{3+} + e^- \rightarrow Ru(bpy)_3^{2+*} \quad (3b)$$

After these excitation steps, $Ru(bpy)_3^{2+*}$ relaxed (reaction (4)) to the ground state inducing the emitted light.

$$Ru(bpy)_3^{2+*} \rightarrow Ru(bpy)_3^{2+} + h\nu \quad (4)$$

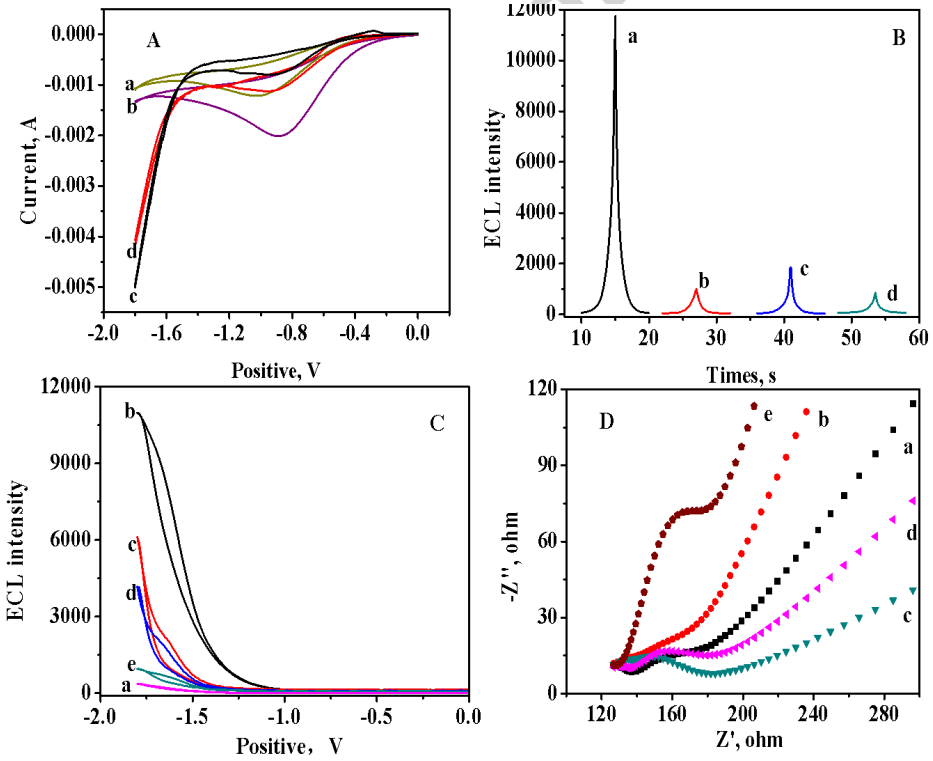

Fig. 3 (A) CV of bare GCE (a), CRuSi-Fe_3O_4/GCE (b), $NiCo_2S_4$-COOH-rGO/GCE (c) and

$NiCo_2S_4$-COOH-rGO/CRuSi-Fe_3O_4/GCE (d) in PBS (pH=8.0) with $K_2S_2O_8$; (B) ECL response of CRuSi-Fe_3O_4/GCE (a), CoS/CRuSi-Fe_3O_4/GCE (b), NiS/CRuSi-Fe_3O_4/GCE (c) and $NiCo_2S_4$-COOH-rGO/GCE (d) in PBS (pH=8.0) containing 0.1 M KCl and 0.1 M $K_2S_2O_8$; (C) ECL profiles of bare GCE (a), CRuSi-Fe_3O_4/GCE (b), Con A/CRuSi-Fe_3O_4/GCE (c), BSA/Con A/CRuSi-Fe_3O_4/GCE (d) and $NiCo_2S_4$-COOH-rGO@Glu/BSA/Con A/CRuSi-Fe_3O_4/GCE (e) in PBS (pH=8.0) containing 0.1 M KCl and 0.1 M $K_2S_2O_8$; (D) EIS of bare GCE (a), CRuSi-Fe_3O_4/GCE (b), Con A/CRuSi-Fe_3O_4/GCE (c), BSA/Con A/CRuSi-Fe_3O_4/GCE (d) and $NiCo_2S_4$-COOH-rGO@Glu/BSA/Con A/CRuSi-Fe_3O_4/GCE (e) in 2.5 mM $Fe(CN)_6^{3-/4-}$ and 0.1 M KNO_3.

The quenching mechanism of $Ru(bpy)_3^{2+}$ and $NiCo_2S_4$-COOH-rGO may be due to ECL-RET. Then, FL measurements and ECL were used to verify us infer. As shown in Fig. S7A, pure $Ru(bpy)_3^{2+}$ showed maximal emission at 621 nm upon excitation at 400 nm in aqueous solution. However, as shown in Fig, 1B, when the equal concentration of NiS (curve a), CoS (curve b), $NiCo_2S_4$ (curve c) and $NiCo_2S_4$-COOH-rGO (curve d) were mixed with the equal concentration of $Ru(bpy)_3^{2+}$, the FL intensity dramatically decreased and the quenching behavior of $NiCo_2S_4$-COOH-rGO was optimal which was consistent with the results of ECL measurements (Fig. 3B). Therefore, according to the published work and our experiments results, the quenching mechanism of $Ru(bpy)_3^{2+}$ and $NiCo_2S_4$-COOH-rGO may be due to ECL-RET. Furthermore, as shown in Fig. 3B, ECL results also indicated that $NiCo_2S_4$-COOH-rGO (curve d) can quench the ECL of CRuSi-Fe_3O_4 (curve a). Curve b and curve c were the ECL intensity of pure CoS/GCE

and NiS/GCE, respectively. When Co(II) and Ni(II) coexisting, the quenching efficiency was optimal. Based on this, the principle of the developed biosensor was that different concentrations of captured Con A which immobilized on CRuSi-Fe_3O_4 using glutaraldehyde as the coupling agent can combine with different quantity of $NiCo_2S_4$-COOH-rGO@Glu through a specific carbohydrate-Con A interaction, leading to the ECL signal of CRuSi-Fe_3O_4 decreased-degree different which was determined by the quantity of $NiCo_2S_4$-COOH-rGO@Glu on the fabricated biosensor.

3.3. ECL and EIS characterization of the biosensor fabrication

The corresponding ECL-potential profiles of the modified-electrodes fabrication process were shown in Fig. 3C, carried out in 0.1 M $K_2S_2O_8$ and 0.1 M KCl. The bare GCE produced a weak ECL (curve a) and it was the ECL of $S_2O_8^{2-}/O_2$ system. When GCE was modified by CRuSi-Fe_3O_4, a remarkable ECL increase was observed compared with bare GCE (curve b). After Con A and BSA were immobilized on the modified electrode, the ECL intensity decreased successively because they both hindered the electron-transfer between $S_2O_8^{2-}$ and luminescent reagents (curve c and curve d) (Wang et al. 2012). Finally, when the resultant biosensor was incubated with $NiCo_2S_4$-COOH-rGO@Glu (curve e), the ECL intensity was decreased remarkably. The reason for this was that $NiCo_2S_4$-COOH-rGO@Glu could effectively quench the ECL of CRuSi-Fe_3O_4. The results indicated that the ECL biosensor was successfully fabricated.

To gain better understanding of fabrication process of the ECL biosensor,

electrochemical impedance spectroscopy (EIS) was also performed at different modified-electrodes in 2.5 mM $[Fe(CN)_6]^{3-/4-}$ and 0.1 M KNO_3. EIS curves of the GCE at different modification steps were shown in Fig. 3D. The bare GCE exhibited a small semicircle domain (curve a), which attributed to a free electron-transfer process. When CRuSi-Fe_3O_4 was modified onto the GCE, the modified GCE presented the smaller semicircle domain (curve b) which indicated that faster electron transfer resistance of $[Fe(CN)_6]^{3-/4-}$ on CRuSi-Fe_3O_4/GCE. After successive assembling of Con A, BSA and $NiCo_2S_4$-COOH-rGO@Glu on the modified electrode, the semicircle domains were all increased (curves c, d and e, respectively). The reason was that the formed protein layer acted as the inert electron and mass-transfer blocking layer, and they significantly hindered the diffusion of ferricyanide toward the electrode surface (Hong et al. 2015; Zhang et al. 2016b). These results indicated that the ECL biosensor was successfully fabricated.

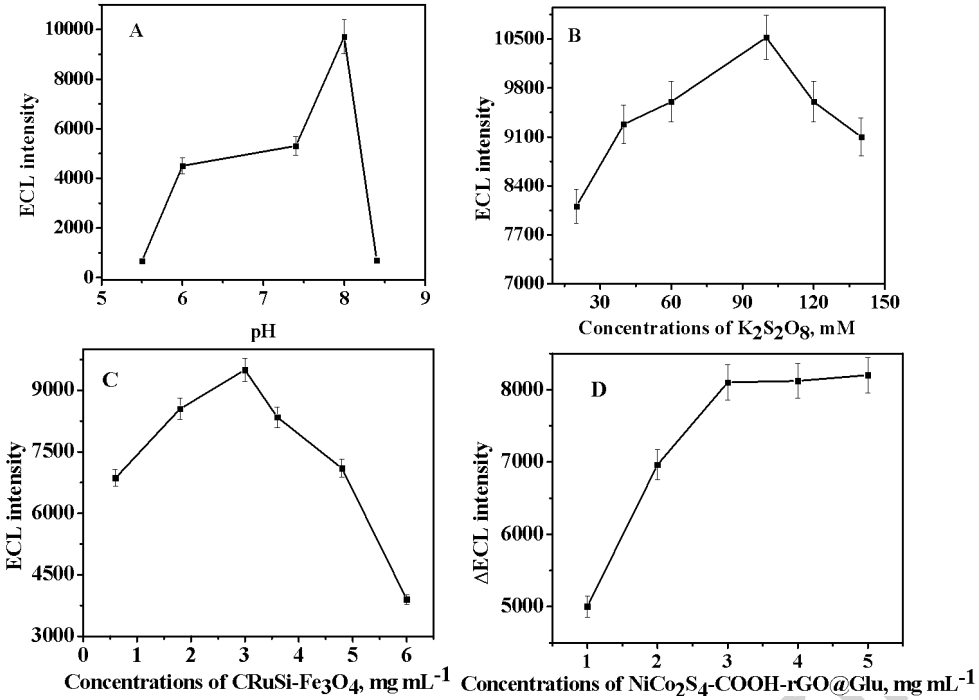

Fig. 4 The effect of pH (A), $K_2S_2O_8$ (B) and CRuSi-Fe_3O_4 (C) on the response of ECL intensity from GCE/CRuSi-Fe_3O_4. (D) The effect of $NiCo_2S_4$-COOH-rGO@Glu concentrations on the ECL biosensor for detection 0.1 ng mL^{-1} Con A (ΔECL intensity was the difference between CRuSi-Fe_3O_4/GCE and $NiCo_2S_4$-COOH-rGO@Glu/BSA/Con A/CRuSi-Fe_3O_4/GCE). Error bars = RSD (*n*=3).

3.4. Optimization of experimental conditions

Experiment conditions had a significant effect on the ECL behavior of CRuSi-Fe_3O_4, such as pH and concentration of coreactant $K_2S_2O_8$, CRuSi-Fe_3O_4 and $NiCo_2S_4$-COOH-rGO@Glu. The pH influence from 5.5 to 8.5 on the biosensor performance was investigated. As described in Fig. 4A, the maximum ECL response appeared at pH 8.0. The reason was that at low pH, the proton could be reduced easily at negative potential and the luminescence was inhibited. What's more, the strong oxidant $SO_4^{\bullet-}$ was consumed at high pH via the scavenging effect of OH^- (Xu and

Dong 2000; Yao et al. 2008). Moreover, highly acidic or alkaline surroundings could damage the immobilized protein. As shown in Fig. 4B, when the concentration of $K_2S_2O_8$ was 100 mM, the ECL intensity of CRuSi-Fe_3O_4 achieved a maximum value. The increase of $K_2S_2O_8$ concentrations would promote the produce of $SO_4^{\bullet-}$, which could oxidize the CRuSi-Fe_3O_4 to form active state CRuSi-Fe_3O_4* (Li et al. 2015). However, further increase of $K_2S_2O_8$ concentration caused the decrease of ECL intensity which is ascribed to that the excess $S_2O_8^{2-}$ would inhibit the producing of excited state of $Ru(bpy)_3^{2+}$ (Cheng et al. 2012a). The concentrations of CRuSi-Fe_3O_4 for fabrication of biosensor was investigated. Fig. 4C depicted the ECL intensity of various concentrations of CRuSi-Fe_3O_4-modified GCE. The ECL intensity increased with the increasing concentrations of CRuSi-Fe_3O_4 (0.5-3 mg mL^{-1}) and then decreased with further increase concentrations of CRuSi-Fe_3O_4, attributing to the self-absorption effect of the luminophor (Hua et al. 2009). As a result, 3 mg mL^{-1} CRuSi-Fe_3O_4 was chosen for fabricating biosensor. In addition, the concentrations of $NiCo_2S_4$-COOH-rGO@Glu for fabricating biosensor was also investigated. Fig. 4D depicted the ECL emission of the biosensor for detection of 0.1 ng mL^{-1} Con A. When the concentrations of luminophor CRuSi-Fe_3O_4 was equal, the ECL intensity changed with the concentrations of $NiCo_2S_4$-COOH-rGO@Glu. When the concentrations of $NiCo_2S_4$-COOH-rGO@Glu was 3 mg mL^{-1}, the ECL difference between CRuSi-Fe_3O_4/GCE and $NiCo_2S_4$-COOH-rGO@Glu/BSA/Con A/CRuSi-Fe_3O_4/GCE reached a platform, thus 3 mg mL^{-1} $NiCo_2S_4$-COOH-rGO@Glu was chosen as the optimal concentration.

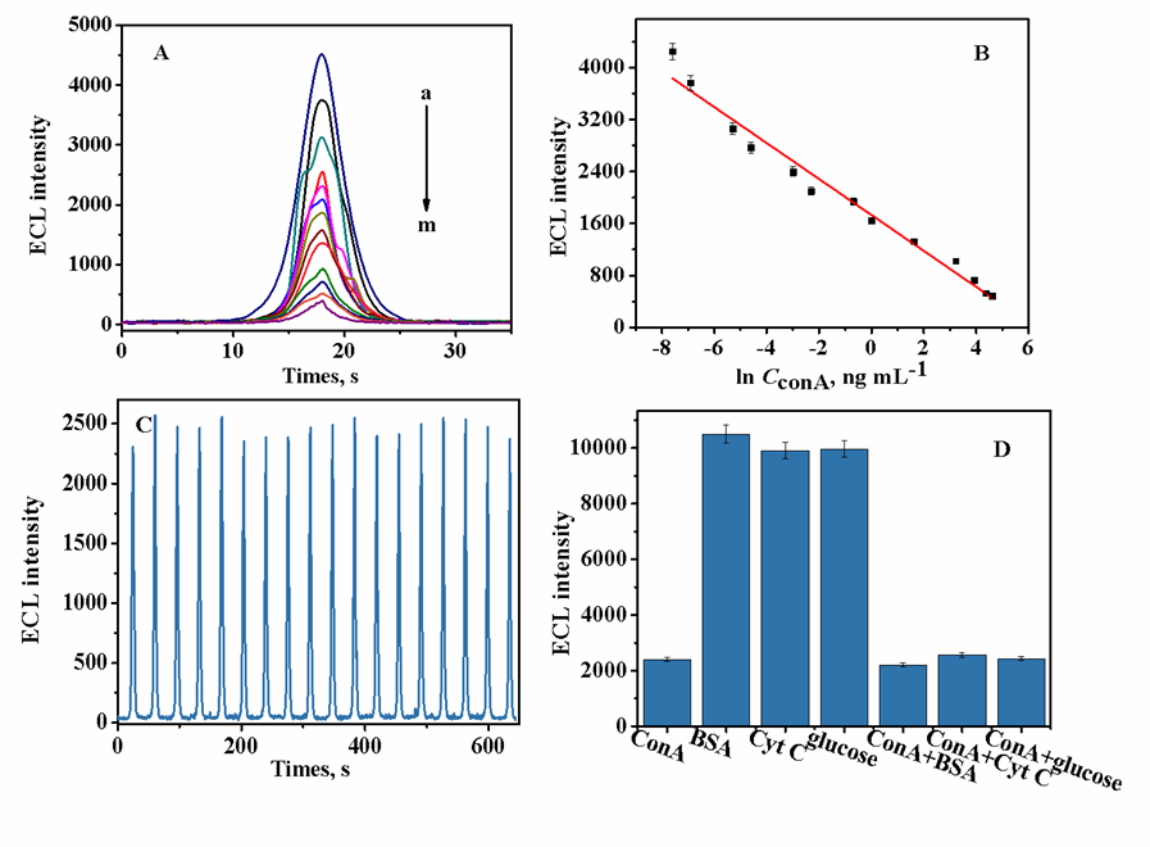

Fig. 5 (A) ECL response of the biosensor to different concentrations of Con A, from a to m: 0.00005, 0.0001, 0.005, .0.01, 0.05, 0.1, 0.5, 1, 5, 25, 50, 80 and 100 ng mL^{-1}. (B) Calibration curve of the biosensor for different concentrations of Con A. (C) Stability of ECL emissions under continuous scanning for 18 cycles in PBS (pH=8.0) containing 0.1 M KCl and 0.1 M $K_2S_2O_8$ for detection of 0.05 ng mL^{-1} Con A. (D) The ECL intensity responses of the biosensors to 0.05 ng mL^{-1} Con A, 0.05 ng mL^{-1} interferences and 0.05 ng mL^{-1} Con A with 10 ng mL^{-1} interferences. Error bars = RSD (n=3).

3.5. Performance of the biosensor

The analytical performance of the proposed biosensor was investigated by incubating with different concentrations of Con A under the optimization conditions. As shown in Fig. 5A, the ECL signals decreased with the increasing concentrations of

Con A from 0.5 pg mL^{-1} to 100 ng mL^{-1} (curve a-m). The obtained ECL intensity was correlated with the exponential value of Con A concentrations and a linear response range from 0.5 pg mL^{-1} to 100 ng mL^{-1} was achieved. As shown in Fig. 5B, the linear equation was I = -276.93ln c + 1731.52, with a correlation coefficient of 0.9871 and a detection limit of 0.18 pg mL^{-1} (S/N = 3). Compared with previous works, the proposed biosensor showed more excellent detection limit and liner range, as shown in Table S1. This suggested that this strategy is highly sensitive and has a great potential for accurate detection of Con A.

3.6. Stability, selectivity and reproducibility of the developed biosensor

Operation stability is one of the main points for extending potential application in the sensing field. Fig. 5C displayed ECL emission of the biosensor for detection of 0.05 ng mL^{-1} Con A under 18 cycles of continuous potential scans. The ECL intensity of the biosensor was pretty stable with the relative standard deviation of 3.08%, which indicated that the sensing signal was quite reliable.

To examine the specificity of the developed biosensor, interferences study was investigated by using BSA, cytochrome C (Cyt C) and glucose. To investigate the non-specificity adsorption of the biosensor, the equal concentration of BSA, Cyt C and glucose was used to replace Con A. As shown in Fig. 5D, no obvious change of ECL intensity was observed in the detection of BSA, Cyt C and glucose in comparison with the blank test. Two hundred times of the above interferences were

added into a 0.05 ng mL^{-1} of Con A solution to investigate the specificity of the biosensor and the RSD of the measurements was 2.71%, indicating that the selectivity of the biosensor was satisfying.

The reproducibility of the biosensor was also investigated by fabrication of seven same electrodes. The RSD of measurements was under 5% for the detection 0.05 ng mL^{-1} Con A, indicating the well reproducibility.

3.7. Application of the developed biosensor

The practical applicability of the designed biosensor was studied by detecting Con A in human serum samples using a standard addition method. From results in Table 1, the recoveries were ranging from 99% to 105%, demonstrating the practicability of designed biosensor for Con A detection in real biological samples.

Table 1 determination of Con A added in human serum samples with the developed biosensor.

Samples	Added (ng mL^{-1})	Found (n=5, ng mL^{-1})	RSD (%)	Recover(%)
Human serum	10.0	10.3	2.5	100.3
	5.0	4.98	2.2	99.56
	1.0	1.05	2.6	105.0

4. Conclusion

In summary, a novel quenching ECL biosensor was developed for detection of Con A. Our results demonstrated that the synthesized CRuSi-Fe_3O_4 exhibited excellent and stable ECL signals. After $NiCo_2S_4$-COOH-rGO@Glu incubated on the modified electrode via the specific carbohydrate-Con A interaction, the ECL intensity decreased

remarkably. The possible quenching mechanism of $Ru(bpy)_3^{2+}$ and $NiCo_2S_4$-COOH-rGO may be due to ECL-RET. The fabricated biosensor exhibited good stability, accuracy and acceptable reproducibility, which suggesting its potential applications in real samples.

Acknowledgements

This study was supported by the Natural Science Foundation of China (No. 21375047, 21377046, 21575050, 21505051), the Science and Technology Plan Project of Jinan (No. 201307010), the Science and Technology Development Plan of Shandong Province (No. 2014GSF120004), the Special Project for Independent Innovation and Achievements Transformation of Shandong Province (2014ZZCX05101), and QW thanks the Special Foundation for Taishan Scholar Professorship of Shandong Province and UJN (No. ts20130937).

References

Cheng, C., Huang, Y., Tian, X., Zheng, B., Li, Y., Yuan, H., Xiao, D., Xie, S., Choi, M.M., 2012a. Analytical Chemistry 84, 4754-4759.

Cheng, C., Huang, Y., Tian, X., Zheng, B., Li, Y., Yuan, H., Xiao, D., Xie, S., Choi, M.M.F., Chem., A., 2012b. Analytical Chemistry 84, 4754-4759.

Dang, J., Guo, Z., Zheng, X., 2014. Analytical Chemistry 86, 8943-8950.

Dennany, L., Forster, R.J., Rusling, J.F., 2003. Journal of the American Chemical Society 125, 5213-5218.

Greenway, G., Greenwood, A., Watts, P., Wiles, C., 2006. Chemical communications 85-87.

Guo, Z., Dong, S., 2004. Analytical chemistry 76, 2683-2688.

Guo, Z., Shen, Y., Zhao, F., Wang, M., Dong, S., 2004. Analyst 129, 657-663.

Hone, D.C., And, A.H.H., Russell, D.A., 2003. Langmuir 19, 7141-7144.

Hong, L.R., Chai, Y.Q., Zhao, M., Liao, N., Yuan, R., Zhuo, Y., 2015. Biosensors & bioelectronics 63C, 392-398.

Hua, L., Han, H., Chen, H., 2009. Electrochimica Acta 54, 1389-1394.
Huang, C.C., Chen, C.T., Shiang, Y.C., Lin, Z.H., Chang, H.T., 2009. Analytical Chemistry 81, 875-882.
Huang, C.F., Yao, G.H., Liang, R.P., Qiu, J.D., 2013. Biosensors & bioelectronics 50, 305-310.
Li, X., Yu, S., Tao, Y., Yong, Z., Du, B., Wu, D., Qin, W., 2016a. Biosensors & bioelectronics
Li, Y., Zhang, S., Dai, H., Hong, Z., Lin, Y., 2016b. Sensors & Actuators B Chemical 232, 226-233.
Liu, B., Zhang, B., Chen, G., Yang, H., Tang, D., 2014. Analytical Chemistry 86, 7773-7781.
Liu, Q., Jin, J., Zhang, J., 2013. Acs Applied Materials & Interfaces 5, 5002-5008.
Loaiza, O.A., Lamasardisana, P.J., Jubete, E., Ochoteco, E., Loinaz, I., Cabañero, G., García, I., Penadés, S., 2011. Analytical Chemistry 83, 2987.
Ma, D.-L., Chan, D.S.-H., Leung, C.-H., 2014. Accounts of chemical research 47, 3614-3631.
Mallakpour, S., Zadehnazari, A., 2013. Polymer 54, 6329-6338.
Marcano, D.C., Kosynkin, D.V., Berlin, J.M., Sinitskii, A., Sun, Z., Slesarev, A., Alemany, L.B., Lu, W., Tour, J.M., 2010. ACS nano 4, 4806-4814.
Qiao, L., Jin, J., Zhang, J., 2013. ACS applied materials & interfaces 5, 5002-5008.
Sardesai, N.P., Barron, J.C., Rusling, J.F., 2011. Analytical chemistry 83, 6698-6703.
Wang, H., Yuan, R., Chai, Y., Niu, H., Cao, Y., Liu, H., 2012. Biosensors & bioelectronics 37, 6-10.
Wang, Y., Li, B., Zhang, L., Song, H., 2013. Langmuir 29, 1273-1279.
Wei, H., Wang, E., 2008. Analytical Chemistry 80, 2250-2254.
Wu, T.S., Li, S.Y., Weng, S.W., Tsiang, C.C., 2012. Polymer 53, 2347-2355.
Xu, G., Dong, S., 2000. Electroanalysis 12, 583-587.
Yang, H., Yang, X.H., Chen, Y.Q., Pan, M., 2009. Chinese Journal of Analytical Chemistry 37, 275-278.
Yao, W., Wang, L., Wang, H., Zhang, X., 2008. Electrochimica Acta 54, 733-737.
Yu, F., Tan, X., Xin, O., Chen, S., Wei, S., 2017. Biosensors & bioelectronics 87, 802-806.
Zhang, X., Tan, X., Zhang, B., Miao, W., Zou, G., 2016a. Analytical Chemistry 88,
Zhang, X., Zhang, B., Miao, W., Zou, G., 2016b. Analytical Chemistry 88,
Zhou, X., Zhu, D., Liao, Y., Liu, W., Liu, H., Ma, Z., Xing, D., 2014. Nature Protocols 9, 1146-1159.
Zhu, D., Zhou, X., Xing, D., 2010. Biosensors & bioelectronics 26, 285-288.

Highlights

1. ECL behavior of Chitosan/$Ru(bpy)_3^{2+}$/silica/Fe_3O_4 nanomaterials was investigated.
2. The ECL of CRuSi-Fe_3O_4 can be quenched by $NiCo_2S_4$-COOH-rGO.
3. $NiCo_2S_4$-COOH-rGO@Glu links with Con A via specific carbohydrate-Con A interaction.